SAND2017-11868J

ORIGINAL ARTICLE

Predicting Large-scale Effects During Cookoff of Plastic-Bonded Explosives (PBX 9501, PBX 9502, and LX-14)

M. L. Hobbs, *,[1] M. J. Kaneshige,[1] W. W. Erikson[1]

Abstract We have made reasonable cookoff predictions of large-scale explosive systems by using pressure-dependent kinetics determined from small-scale experiments. Scale-up is determined by properly accounting for pressure generated from gaseous decomposition products and the volume that these reactive gases occupy, e.g. trapped within the explosive, the system, or vented. The pressure effect on the decomposition rates has been determined for different explosives by using both vented and sealed experiments at low densities. Low-density explosives are usually permeable to decomposition gases and can be used in both vented and sealed configurations to determine pressure-dependent reaction rates. In contrast, explosives that are near the theoretical maximum density (TMD) are not as permeable to decomposition gases, and pressure-dependent kinetics are difficult to determine. Ignition in explosives at high densities can be predicted by using pressure-dependent rates determined from the low-density experiments as long as gas volume changes associated with bulk thermal expansion are also considered. In the current work, cookoff of the plastic-bonded explosives PBX 9501 and PBX 9502 is reviewed and new experimental work on LX-14 is presented. Reactive gases are formed inside these heated explosives causing large internal pressures. The pressure is released differently for each of these explosives. For PBX 9501, permeability is increased and internal pressure is relieved as the nitroplasticizer melts and decomposes. Internal pressure in PBX 9502 is relieved as the material is damaged by cracks and spalling. For LX-14, internal pressure is not relieved until the explosive thermally ignites. The current paper is an extension of work presented at the 26th ICDERS symposium [1].

Keywords Cookoff, PBX 9501, PBX 9502, LX-14, scale-up, pressure-dependent

1 Introduction

Violence in cookoff accidents often involves shocks in degraded energetic materials. The focus of the current paper is on the state of the degraded materials during cookoff of plastic bonded explosives, which is a major unsolved problem. In the current work, we discuss cookoff of three plastic-bonded explosives: PBX 9502, PBX 9501, and LX-14. PBX 9502 is composed of 95 wt% triaminotrinitrobenzene (TATB) and 5 wt% chlorotrifluoro-ethylene/vinylidine fluoride (Kel-F). PBX 9501 is composed of 95 wt% octahydro-1,3,5,7-tetranitro-1,3,5,7-tetrazocine (HMX) and 2.5 wt% Estane® 5703 (a polyurethane thermoplastic), and 2.5 wt% of a nitroplasticizer (NP): BDNPAF, a 50/50 wt% eutectic mixture of bis(2,2-diniropropyl)-acetal (BDNPA) and bis(2,2-dinitropropyl)-formal (BDNPF). LX-14 is composed of 95.5 wt% HMX and 4.5 wt% Estane® 5702-F1.

* mlhobbs@sandia.gov, 505-844-5988
[1] Sandia National Laboratories, Albuquerque, NM 87111 USA

The cookoff characteristics of each of these explosives was observed in Sandia's Instrumented Thermal Ignition (SITI) experiment, which is shown schematically in Fig. 1. Explosives in SITI normally consist of two 2.54-cm diameter by 1.27-cm high cylinders confined by aluminum. Nine thermocouples, located at various radial position indicated in Fig. 1.c, are inserted between these two cylinders of explosives. The small air gap above the explosive in Fig. 1.a is for thermal expansion. This air gap is connected to a pressure transducer by 41-cm of tubing. The larger air gap in Fig. 1.b accommodates a borescope that is used to observe *in situ* decomposition of the PBXs. The primary SITI observations are internal temperatures, pressure, and ignition time.

We have previously published detailed cookoff models for PBX 9501 [2] and PBX 9502 [3]. The kinetics for these models were obtained from SITI data using 10-20 g of explosive in both vented and sealed configurations. The models were then validated using experiments that used substantially larger explosive mass. For example, the predictive capability of the PBX 9501 model was successfully validated with experiments from five other laboratories with explosive masses ranging from 2 g to more than 2.5 kg of explosive [2]. Similarly, the predictive capability of our PBX 9502 model was evaluated with "blind" comparisons to tests using 1.3 kg of PBX 9502 at Los Alamos National Laboratory (LANL) [4]. The "blind" predictions were performed before the tests were run.

We believe the ability of our PBX 9501 and PBX 9502 models to predict cookoff response in substantially larger systems than the SITI experiments is due to the inclusion of at least one pressure-dependent reaction. In our models, we solve the conductive energy equation with a source term for thermal decomposition. We can confidently predict ignition in low-density explosives since the permeability is high. In contrast, predicting ignition in high-density explosives is difficult since the porosity within the explosive is either closed, partially closed, or open. The measured ignition time is normally bounded by our open-pore and closed-pore predictions.

More accurate ignition predictions in fully-pressed explosives can be made by understanding the mechanism by which decomposition gases leave the high-density explosive. The remainder of this paper describes and presents experimental evidence of how decomposition gases leave the high-density explosives. In the current work, we examine three plastic-bonded explosives that release decomposition gases in different ways. The differences are related to the specific binder.

2 Damage Mechanisms in PBX 9502

Pristine samples of PBX 9502 are shown in Figures 2.a. The left image shows molding powder or prills of PBX 9502; the middle image shows a pressed sample that is near TMD; and the right image shows degraded PBX 9502 that was initially at 98% TMD and heated to 530 K.

Decomposition gases are less likely to be trapped within the explosive prills than in the fully pressed explosive. In fact, decomposition gases accumulating within the highly pressed explosive are at higher pressures and can abruptly fracture the PBX 9502 as shown in Fig. 2.b and 2.c.

Figure 2.b shows three video frames from an open half shell SITI experiment. The left image in Fig. 2.b shows the 2.54-cm diameter by 1.27-cm high cylinder of PBX 9502 being heated. Internal pressure builds as decomposition products accumulate within the PBX 9502 sample. Eventually an audible "bang" was recorded as material was expelled out of the middle of the explosive as shown in the center image in Fig. 2.b. Yellow gas is seen leaving the crater in this image. Towards the end of the video, white gas leaves the crater and PBX 9502 conductively burns as shown by the orange glow in the right image in Fig. 2.b. Room temperature PBX 9502 does not normally burn in this fashion at atmospheric pressure.

We attempted to restrain the PBX 9502 from being expelled from the explosive by using a

washer as shown in the left image in Fig. 2.c. Instead of creating a pressure relieving crater, the explosive cracked, spalled, and flaked as shown in the middle image of Fig. 2.c. Eventually a smaller crater was abruptly formed to relieve the internal pressure and white smoke was observed as presented in the right image in Fig. 2.c

Figure 2.d presents further evidence of mechanical damage and relief of trapped decomposition gas. The left image in Fig. 3.d shows the measured pressure from two experiments 280s (high-density) and 225s (low-density). The test numbers are appended with either "s", "v", or "vb" representing sealed, vented and vented experiments with borescope, respectively.

During experiment 280s, various noises were recorded and correspond to an abrupt change in pressure. We believe the noises and unsteady pressure are evidence of material damage as internal pressure builds and is relieved. Similar noises and abrupt pressure changes were not observed during decomposition of the lower density explosive test 225s.

The right image in Fig. 2.d shows the temperature recorded with the nine radial thermocouples in blue. The red line is the temperature of the confining aluminum. The black line represents the measured pressure. There is a temperature excursion prior to the final ignition. The sudden increase in pressure during the temperature excursion is caused by release of internal gases into the expansion volume and pressure tubing. More information regarding the PBX 9502 experiments and models can be found in [3].

3 Damage Mechanisms in PBX 9501

Our PBX 9501 experiments showed a reactant-limited exotherm during our low-density vented experiments as shown in Fig. 3.a and labelled as a "Temperature excursion". We associated this reactant-limited exotherm with decomposition of the nitroplasticizer in the binder. We did not observe the reactant-limited exotherm with our low-density *sealed* experiments as shown in Fig. 3.b. In Fig. 3, the center thermocouple is red.

The reactant-limited exotherm was not observed during our vented and sealed high-density experiments as shown in Fig 3.c. We believe the nitroplasticizer may have extruded to the surface of the explosive and decomposed near the highly conductive confining aluminum since the nitroplasticizer has a higher expansion coefficient than HMX. The nitroplasticizer was not a factor in the ignition time for these high-density experiments.

Thermal damage in PBX 9501 is significantly different than in PBX 9502. Rather than cracking and spalling as shown for PBX 9502 in Fig. 2.c, the NP in PBX 9501 melts and decomposes. This increases the permeability of the PBX and provides a pathway for internally generated decomposition gases to leave the explosive.

Figure 4.a shows pristine PBX 9501. The left image shows low-density prills or molding powder; the middle image shows PBX 9501 that was pressed to 85% TMD, and the right image shows PBX 9501 pressed to 96% TMD. Similar pristine LX-14 samples are shown in Fig. 4.b. Thermally damaged PBX 9501 is shown in Fig. 4.c.

Each of the images in Fig. 4.c was taken with a borescope camera just prior to ignition. Not much of the plasticizer is extruded in the 85% TMD samples shown in the left and middle images. Although the vented experiment shown on the left has a little more extruded plasticizer than the sealed system shown in the middle image.

A substantial amount of plasticizer is extruded from the high-density PBX 9501 sample shown in the right image of Fig. 4.c. The mechanism for increased permeability in degraded PBX 9501 is related to the easy removal of the plasticizer as opposed to mechanical damage in PBX 9502. Contrasting the cookoff behavior of PBX 9501 and PBX 9502 emphasizes the effect of the binder and *retention* or *release* of reactive decomposition products during cookoff.

We performed additional cookoff experiments with LX-14 to confirm the effect of the nitroplasticizer on cookoff of PBX 9501. LX-14 has about the same amount of HMX as PBX 9501, has an Estane binder, but does not have nitroplasticizer. We expected PBX 9501 to ignite sooner than the LX-14 due to the reactive nitroplasticizer. However, we measured the *opposite trend*: LX-14 ignited sooner than PBX 9501. The following section highlights the differences between cookoff of PBX 9501 and cookoff of LX-14 using experimental evidence.

3 Damage Mechanisms in LX-14

Figures 4.b and Fig 4.d show pristine and heated LX-14. Some of the prills are dyed purple for easy identification. The pristine PBX 9501 in Fig 4.a are similar to the pristine LX-14 in Fig 4.b, except for the color.

Figure 4.d shows three borescope images at the start, near ignition, and one frame before ignition for test 558vb. The control thermocouple was ramped from 292.8 K to 468.3 K in 600 seconds and then held at 468.3 K. The low-density molding powder ignited after 10482 s.

The middle image in Fig. 4.d seems discolored. We believe the discoloration is caused by condensing decomposition products on the borescope lens. The prills do not move and the dark color around the prills is the shadow of the prills. About 30 frames before ignition, the prills start to move as liquid HMX becomes visible. The right image in Fig. 4.d shows the last borescope frame. Liquid HMX is shown in this image.

Figure 5.a shows the temperature history for test 558vb with the red line representing the center temperature. The melting point of HMX (540 K) is also shown in Fig. 5.a. More details near ignition are shown in Fig. 5. Clearly the temperatures of thermocouples 1-3 and 6 exceed the melting point of HMX. Similar results were not obtained in our PBX 9501 runs since the thermocouples and borescope broke before the HMX melting point was reached.

The right image in Fig. 5.c shows a close-up view of liquid HMX from the last borescope image for run 558vb. The upper image is not annotated for clarity and the lower image is annotated to highlight the ignition point and gases or fluids moving away from this point. The ignition was shown more clearly in the video, but cannot be shown in the current paper.

4 Ignition in LX-14 and PBX 9501

Figure 6.a shows ignition time for LX-14 and PBX 9501 as a function of density and temperature. In Fig. 6.a, the red filled circles represent sealed SITI runs with LX-14 and the white circles represent vented SITI runs with LX-14. The small green and white squares represent sealed and vented SITI runs with PBX 9501, respectively.

The left image shows a large difference in ignition times between vented and sealed experiments with both PBX 9501 and LX-14. This difference is much larger in PBX 9501 than LX-14. For example, the difference in ignition times between vented and sealed LX-14 runs 501s and 502v is 2140s. In contrast, the difference in ignition times between vented and sealed PBX 9501 runs 413s and 414v is 8140 s at the same set point temperature of 478.2 K.

We believe the delay between vented and sealed reactions for both PBX 9501 and LX-14 is caused by a significant gas-phase reaction. The delay in ignition for PBX9501 is about 6000 s longer than for LX-14. The longer ignition times are caused by the reactive gases escaping from PBX 9501 as the plasticizer liquefies, porosity increases, and reaction rates decrease with the lower pressure. In contrast, the Estane binder in LX-14 does not degrade and the reactive gases react faster at the higher internal pressures.

Differences in the ability to retain reactive gases between PBX 9501 and LX-14 are even greater in the higher density SITI runs. In fact, most of the gases are retained within LX-14 for densities greater than 85% TMD as shown in the middle and right images in Fig. 6.a. In these images, the

vented ignition times are fairly close to the sealed ignition times. For example, the difference between the vented and sealed runs 557v and 547s is only 146 s for high-density LX-14 at a set point temperature of 478.3 K.

LX-14 retains reactive gases by the higher strength binder resulting in faster ignition times. In contrast, the nitroplasticizer in the PBX 9501 binder melts and reacts at low temperature, which allows decomposition gases to escape from the interior of the explosive. The disparity between vented and sealed ignition times for PBX 9501 is significantly greater than observed for LX-14. In fact, we see no difference between our vented and sealed ignition times for LX-14 for loading densities higher than 85% TMD, which implies that the Estane binder in LX-14 is not permeable to decomposition gases at higher densities.

5 Summary and Conclusions

Our decomposition models for PBX 9501 and PBX 9502 have been simplified by using pressure-dependent reaction rates, which are a simple way to account for significant gas-phase reactions, without knowing the specific details of the reaction mechanism. The pressure dependency was determined by performing small-scale experiments that were either vented or sealed. Some of these experiments were performed using molding powders to prevent the decomposition gases from being trapped within the explosive. Other experiments were performed with fully pressed explosives. We also performed several experiments with different free gas volume, sometimes referred to as ullage. Furthermore, we used a borescope in some experiments to visually observe the explosive as it decomposed *in situ*.

Understanding the role of the binder in our PBX formulations, such as propensity for damage and reactivity, was necessary to predict cookoff response in large-scale systems. Factors to consider include retention of gas within the explosive, damage of the explosive, gas release into the ullage, and gas leakage from the confining vessel. Knowing the working pressure of the large-scale systems was needed to accurately predict ignition times for these pressure sensitive explosives. The pressure was assumed to be ambient when the confining vessel ruptured or leaked. In the current work, our thermal-chemical models did not consider mechanical failure of the explosive or the confining vessel. In general, our predictions bounded the experimental response by assuming the explosive was either intact (e.g. fully pressed) or fully damaged (e.g. powders).

We have observed a cookoff paradox involving PBX 9501 and LX-14 with nominally the same amount of HMX and an Estane binder. The primary difference between these two explosives is that the PBX 9501 also contains 2.5% nitroplasticizer. We discovered that the LX-14, without the nitroplasticizer, reacted sooner than PBX 9501. We concluded that the difference in ignition times depends on the ability of the explosive to retain reactive gases with LX-14 significantly better than PBX 9501.

6 Future Work

All cookoff mechanisms should consider a drying mechanism, a pressure-dependent reaction step for gas-phase dominant reactions, a pressure-independent reaction step for condensed-phase dominant reactions and other steps unique to the explosive such as the nitroplasticizer reaction for PBX 9501. Models should predict mechanical damage and permeability to increase predictive confidence for high-density explosives exposed to abnormal thermal environments.

Acknowledgements

Sandia National Laboratories is a multi-mission laboratory managed and operated by National Technology and Engineering Solutions of Sandia, LLC., a wholly owned subsidiary of Honeywell International, Inc., for the U.S. Department of Energy's National Nuclear Security Administration under contract DE-NA0003525.

The authors acknowledge the Joint DoD/DOE Munitions Program for partial support of this work. We thank Shane Snedigar for running the SITI experiments and Tyler Voskuilen for finite element code development. We also thank Roy Hogan, Leanna Minier, Tony Geller, and Sophia Lefantzi for their constant interest and enthusiasm regarding our experimental and modeling activities. Our internal reviewers, Cole Yarrington and Marcia Cooper, are also appreciated.

References

1. Hobbs, M.L., Kaneshige, M.J.: Predicting Large-scale Effects During Cookoff of PBXs and Melt-castable Explosives. In: 26th International Colloquium on the Dynamics of Explosions and Reactive Systems, Boston (2017)
2. Hobbs, M.L., Kaneshige, M.J., Erikson, W.W.: Modeling the measured effect of a nitroplasticizer (BDNPA/F) on cookoff of a plastic bonded explosive (PBX 9501). Comb. Flame **173**, 132-150 (2016)
3. Hobbs, M.L., Kaneshige, M.J.: Ignition experiments and models of a plastic bonded explosive (PBX 9502): J. Chem. Phys. **140**, 124203 (2014)
4. Aviles-Ramos, C., Hobbs, M.L., Parker, G.R., Kaneshige, M.J., Holmes, M.D.: Validation of a Pressure Dependent PBX 9502 Cookoff Model. In: 15th International Detonation Symposium, San Francisco (2014)

Figure Captions

Fig. 1 SITI schematic with a) small and b) large expansion gap. c) Cross-section of PBX in the SITI apparatus showing thermocouple locations

Fig. 2 a) Pristine PBX 9501 samples used in SITI apparatus: Left image is molding powder (39% TMD, 0.75 g/cm^3), center image is a pressed pellet (98% TMD, 1.9 g/cm^3), and the right image is a degraded sample that was originally 98% TMD. b) PBX 9502 in SITI half shell configuration: left image is taken just before crater formation, middle image shows large crater evolving yellow smoke, nad right image shows a conductive burn following ignition. c) PBX 9502 pellet constrained with washer in SITI half shell configuration. Left image is at start of heating, middle image is near ignition, and right image is the frame before ignition. d) Pressure from run 280s (98% TMD) and 225s (39% TMD) and temperature and pressure from SITI run 277s (98% TMD)

Fig. 3 Radial temperatures in a) low-density vented, b) low-density sealed, and c) high-density vented and sealed SITI experiments. The red line is the center temperature

Fig. 4 a) Pristine PBX 9501 at various densities, b) pristine LX-14 at various densities, c) borescope images of heated PBX 9501, and d) borescope images of heated LX-14

Fig. 5 a) Complete SITI temperature and b) SITI temperature near ignition at the nine radial locations indicated in Fig. 1.c. c) close-up image of HMX liquid showing ignition

Fig. 6 a) SITI ignition times for PBX 9501 and LX-14. b) SITI temperature history at nine radial locations indicated in Fig. 1.c and pressure profiles

Fig. 1

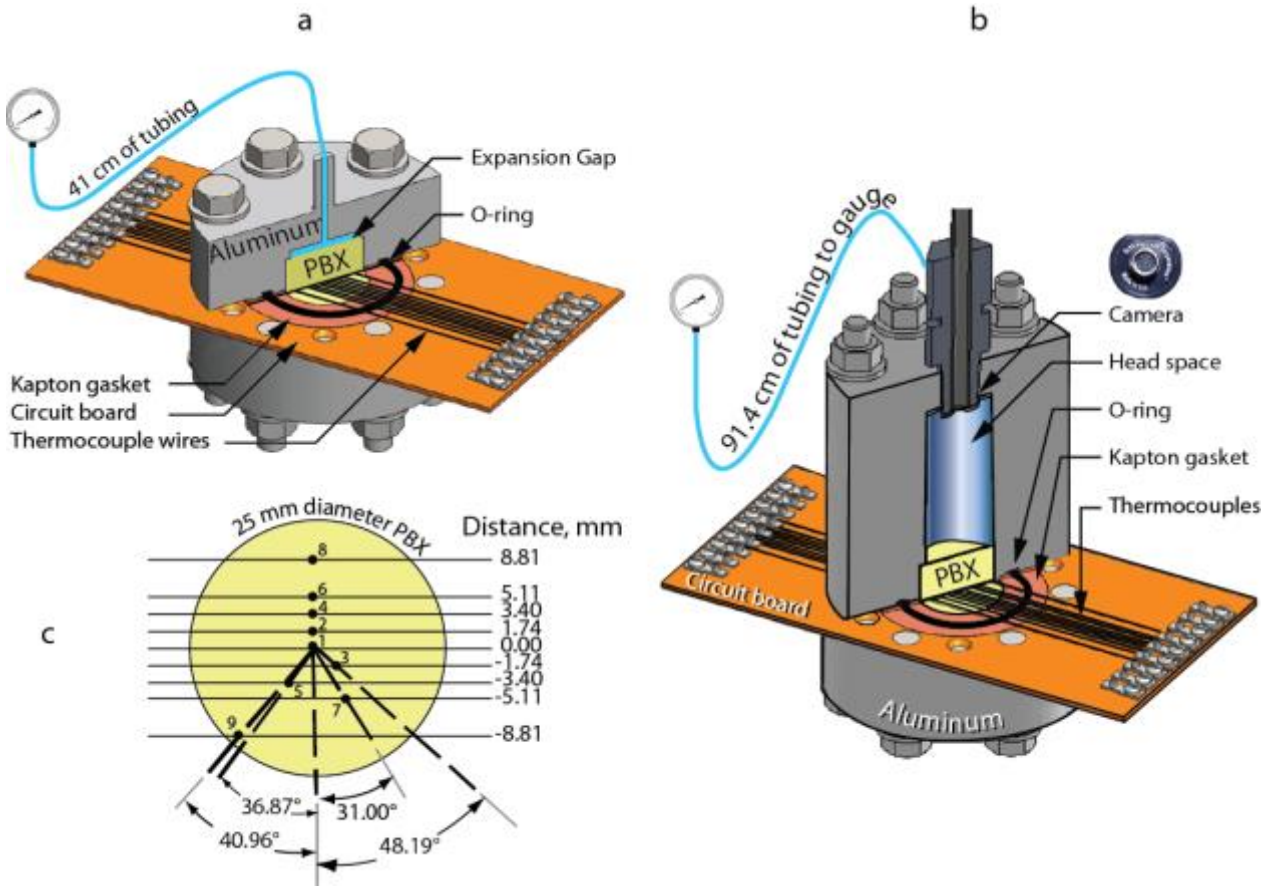
a
41 cm of tubing
Expansion Gap
O-ring
Aluminum
PBX
Kapton gasket
Circuit board
Thermocouple wires
b
91.4 cm of tubing to gauge
Camera
Head space
O-ring
Kapton gasket
Thermocouples
PBX
Circuit board
Aluminum
c
25 mm diameter PBX
Distance, mm
8.81
5.11
3.40
1.74
0.00
-1.74
-3.40
-5.11
-8.81
36.87°
31.00°
40.96°
48.19°

Fig. 2

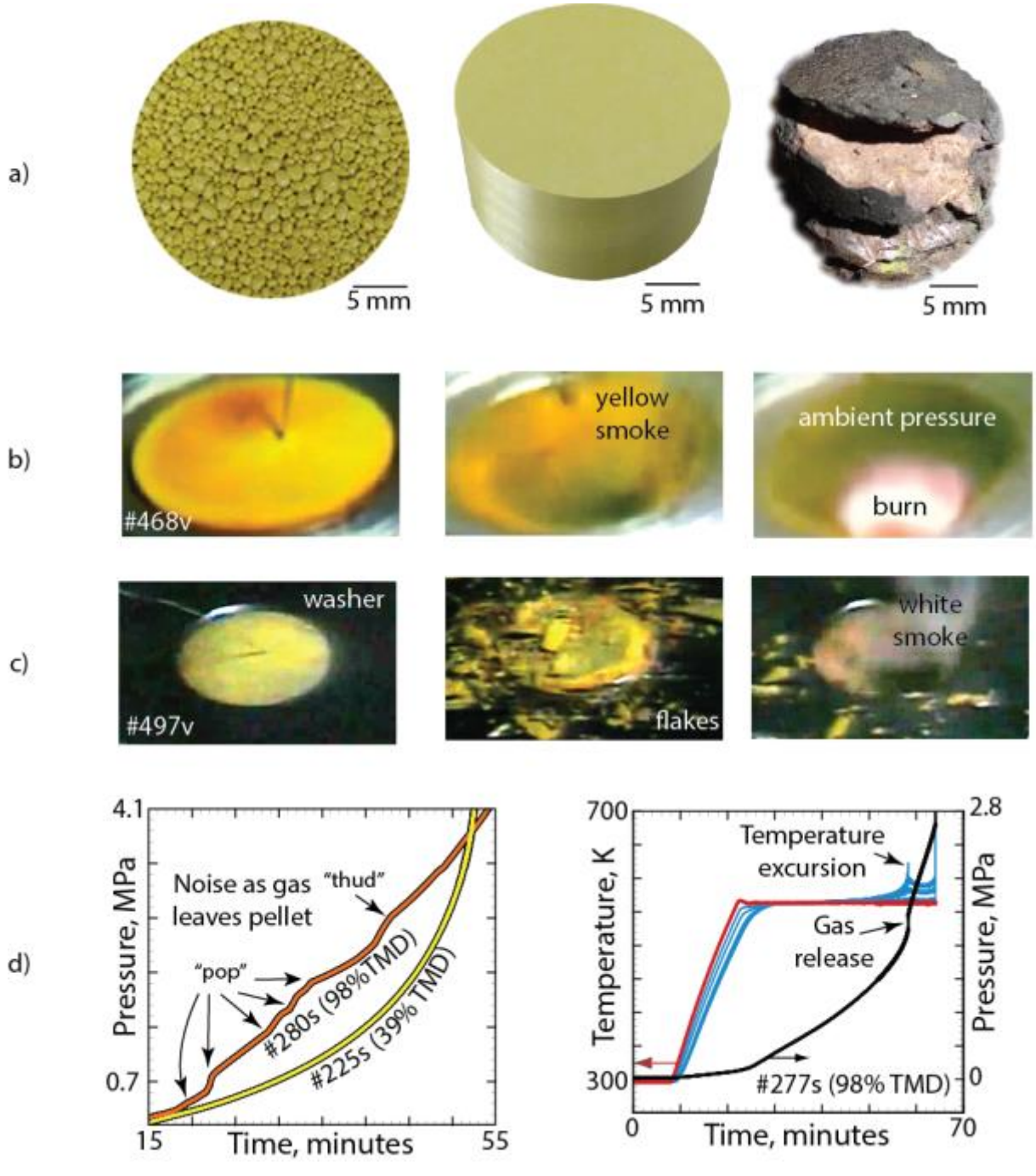
a)
5 mm
5 mm
5 mm
b)
#468v
yellow
smoke
ambient pressure
burn
c)
washer
#497v
flakes
white
smoke
d)
4.1
Pressure, MPa
0.7
Noise as gas
leaves pellet
"thud"
"pop"
#280s (98%TMD)
#225s (39% TMD)
15
Time, minutes
55
700
Temperature, K
300
Temperature
excursion
Gas
release
#277s (98% TMD)
0
Time, minutes
70
2.8
Pressure, MPa
0

Fig. 3

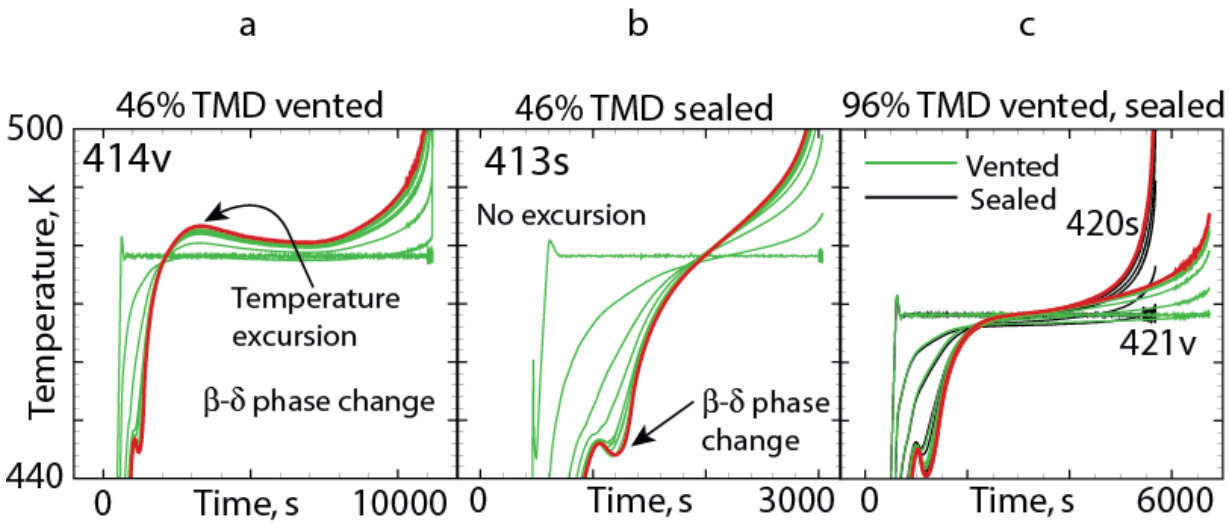
a
b
c
46% TMD vented
46% TMD sealed
96% TMD vented, sealed
500
440
Temperature, K
414v
Temperature
excursion
β-δ phase change
413s
No excursion
β-δ phase
change
Vented
Sealed
420s
421v
0
Time, s
10000
0
Time, s
3000
0
Time, s
6000

Fig. 4

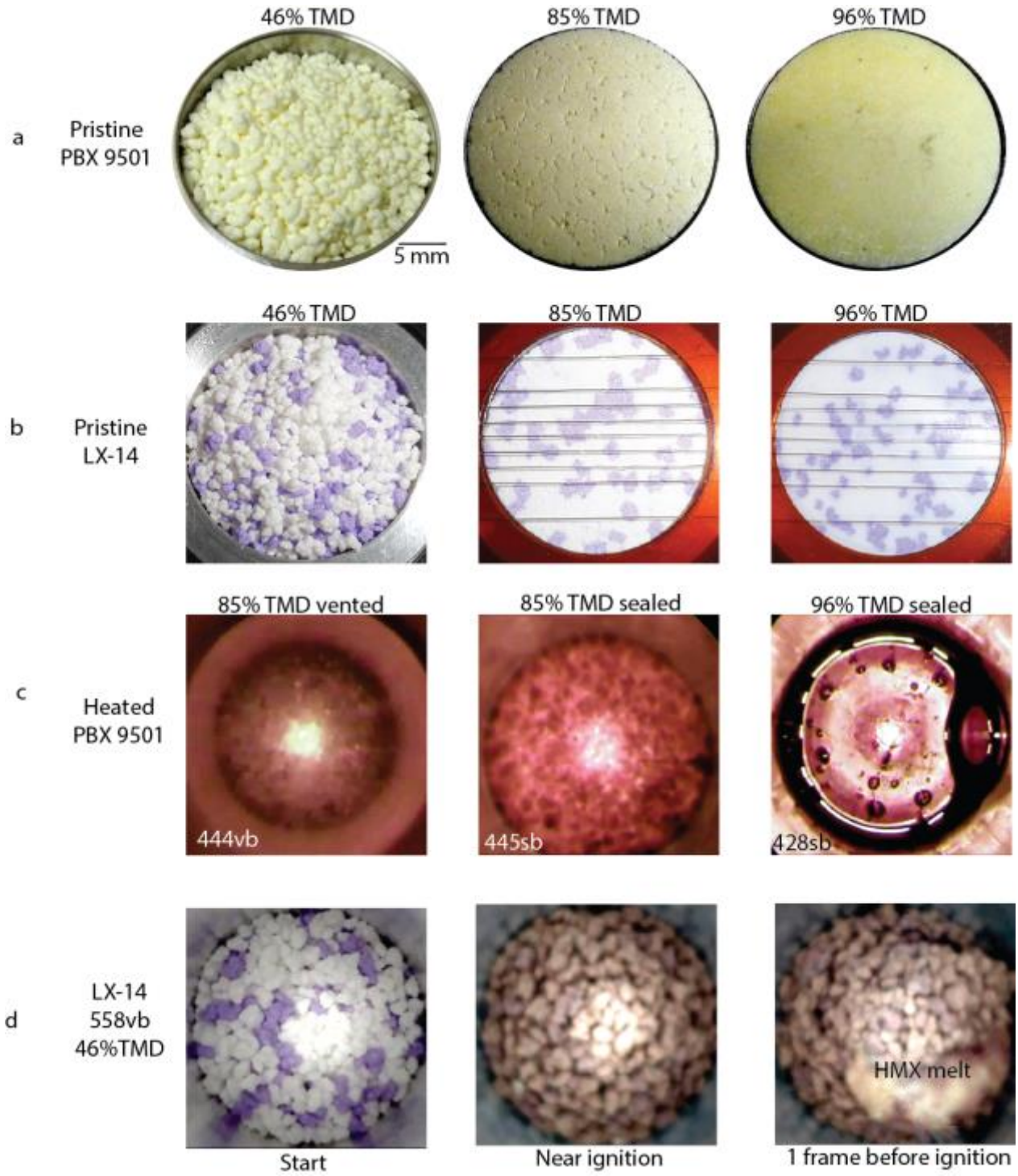
46% TMD
85% TMD
96% TMD
a
Pristine
PBX 9501
5 mm
46% TMD
85% TMD
96% TMD
b
Pristine
LX-14
85% TMD vented
85% TMD sealed
96% TMD sealed
c
Heated
PBX 9501
444vb
445sb
428sb
d
LX-14
558vb
46%TMD
HMX melt
Start
Near ignition
1 frame before ignition

Fig. 5

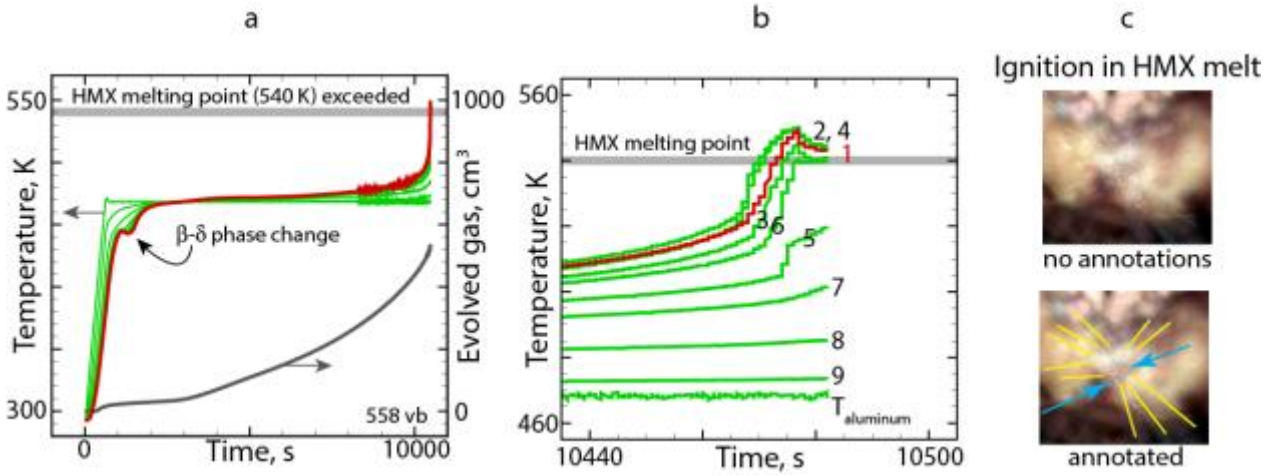
a
b
c
HMX melting point (540 K) exceeded
550
300
1000
0
Temperature, K
Evolved gas, cm³
β-δ phase change
558 vb
0
Time, s
10000
560
460
HMX melting point
2, 4
1
3
6
5
7
8
9
T aluminum
Temperature, K
10440
Time, s
10500
Ignition in HMX melt
no annotations
annotated

Fig. 6

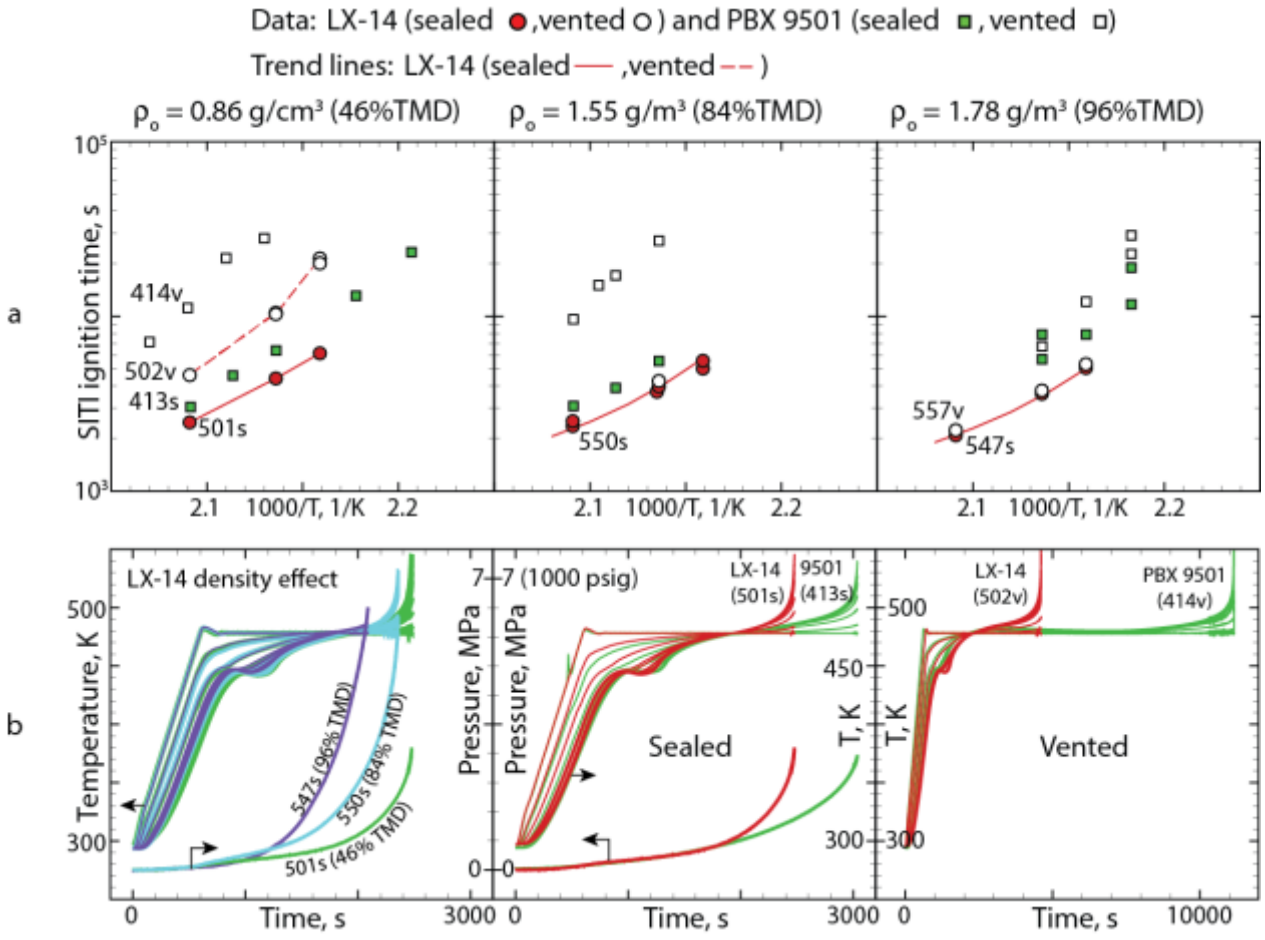
Data: LX-14 (sealed ●,vented ○) and PBX 9501 (sealed ■, vented □)
Trend lines: LX-14 (sealed —, vented – –)
ρo = 0.86 g/cm³ (46%TMD)
ρo = 1.55 g/m³ (84%TMD)
ρo = 1.78 g/m³ (96%TMD)
a
SITI ignition time, s
414v
502v
413s
501s
550s
557v
547s
1000/T, 1/K
b
LX-14 density effect
Temperature, K
547s (96% TMD)
550s (84% TMD)
501s (46% TMD)
Time, s
7 (1000 psig)
Pressure, MPa
LX-14 (501s)
9501 (413s)
Sealed
T, K
LX-14 (502v)
PBX 9501 (414v)
Vented